This article has been accepted for publication in a future issue of this journal, but has not been fully edited. Content may change prior to final publication. Citation information: DOI 10.1109/TOH.2022.3141187, IEEE Transactions on Haptics

The impact of size and position of reference electrode on the localization of biphasic electrotactile stimulation on the fingertips

Milica Isaković, Jovana Malešević, Miloš Kostić, Strahinja Došen, Matija Štrbac

***Abstract*—Development of haptic interfaces to enrich augmented and virtual reality with the sense of touch is the next frontier for technological advancement of these systems. Among available technologies, electrotactile stimulation enables design of high-density interfaces that can provide natural-like sensation of touch in interaction with virtual objects. The present study investigates the human perception of electrotactile sensations on fingertips, focusing on the sensation localization in function of the size and position of reference electrode. Ten healthy subjects participated in the study, with the task to mark the sensations elicited by stimulating the index fingertip using an 8-pad electrode. The test systematically explored several configurations of the active (position) and reference (position and size) electrode pads. The results indicated that there was a spreading of perceived sensations across the fingertip, but that they were mostly localized below the active pad. The position and size of the reference electrode were shown to affect the location of the perceived sensations, which can potentially be exploited as an additional parameter to modulate the feedback. The present study demonstrates that the fingertip is a promising target for the delivery of high-resolution feedback.**

***Index Terms*— Human-Computer Interaction, Perception and Psychophysics, Tactile Display, Virtual Reality.**

I. Introduction

AUGMENTED and virtual reality (AR/VR) technologies are developing at a fast pace and their application expands to different sectors, from gaming to skill training. By generating artificial visual and auditory inputs, these technologies can create a powerful feeling of immersion. However, the user experience can be substantially impaired when they start interacting with the virtual objects, since most VR/AR systems do not provide haptic feedback. The latter is, however, an essential component of human experience, as the haptic feedback is instrumental for grasping, manipulation, exploration of the environment as well as social and affective communication [1], [2]. The restoration of tactile feedback in VR and AR recently receives increasing attention in academia as well as in industry [3]–[5].

Tactile feedback is based on delivering external stimuli to the skin using a variety of actuators (pin arrays, electromagnetic actuators, pneumatic balloons, ultrasound transducers, piezoelectric benders, fabric), but most commonly used are vibrotactile [6] and electrotactile [7] stimulation. These devices are often used as feedback interfaces in AR/VR applications [8], [9], teleoperation [10]–[12], entertainment [13], mobile environment communication [14], [15], as well as for providing missing sensory information from the bionic limbs in prosthetics [16], [17]. Vibrotactile stimulation has been the preferred solution in tactile displays since the late ‘50s, as vibration motors are easy to apply, and there are many applications where sending only the most basic information is sufficient [18]. Technological developments and miniaturization of actuators have led to compact and wearable designs, with numerous motors distributed across palms and fingers and embedded into a glove, [19], [20]. Yu et al. recently presented arrays of millimeter-scale vibratory actuators integrated into soft sheets of electronics that laminate directly onto the skin [21]. Although this approach could improve inherent limitations of vibrotactile technology, including size, resolution, sound, energy consumption and overall scalability of the solution, it is still in the initial phase of development. Additionally, the parameters of vibrotactile stimulation are coupled due to mechanical interaction and resonance effects, and hence cannot be independently modulated [22].

The electrotactile stimulation can overcome some of the existing drawbacks of vibrotactile technology. Electrotactile displays are based on delivering low-intensity electrical current to the skin to activate cutaneous nerve fibers and thereby elicit tactile sensations. These systems are efficient in terms of power consumption, they are simple to fabricate, and provide independent and simultaneous modulation of multiple parameters (e.g., location, amplitude, pulse width and

The work in this study was performed within the TACTILITY project, which has received funding by European Union’s Horizon 2020 framework programme for research and innovation H2020-ICT-2018-2020/H2020-ICT-2018-3 under grant agreement no. 856718.

M. Isaković, J. Malešević, M. Kostić and M. Štrbac are with Tecnalia Serbia Ltd, Deligradska 9/39 11000 Belgrade, Serbia (e-mails: {milica.isakovic} {jovana.malesevic} {milos.kostic} {matija.strbac}@tecnalia.com).

S. Došen is with the Department of Health Science and Technology, Aalborg University, Frederik Bajers Vej 7D 9220 Aalborg Ø, Denmark (e-mail: sdosen@hst.aau.dk).

frequency) [7]. Unlike mechanical vibrators, electrotactile stimulators have no moving parts, and hence they have fast response and allow producing compact displays. The interface can integrate a large number of electrodes, which can be customized in shape, size and configuration. Finally, thanks to high-resolution and independent control of multiple parameters, electrotactile feedback can communicate complex multivariable information in an intuitive manner via appropriately designed dynamic stimulation patterns [23]. On the other side, the electrical stimulation can produce uncomfortable and even painful sensations if the parameters are not properly adjusted.

Fingertips, being the body part with the highest tactile acuity [1], are considered to be the preferred stimulation site for many applications of interest [24]. Successful use of high-density matrix electrodes over the fingertips for eliciting high-fidelity sensations has been reported by several groups [25]–[31], providing a significant amount of evidence that this approach has the potential to unlock the possibilities of tactile communication. Yem and Kajimoto used a 4 × 5 electrode array film (1.5 mm diameter and 2 mm distance) surrounded by a ground electrode [25]. In another study by the same authors, the subject pressed their fingertip over stimulation electrodes arranged as a 3 × 3 array while holding a grounding stick with their thumb [31]. Finger-mounted arrays comprising eight rectangular electrodes (2.5 mm × 1.25 mm) surrounded by the common ground were used to provide haptic perception in VR [26]. Using a similar setup including 2 × 3 matrix of 3 mm × 4 mm pads and a surrounding common ground, we have recently investigated the relation between stimulation amplitude and stimuli localization, which is of crucial importance for defining the procedures for the tactile stimuli calibration [32]. Micro-needle electrode array proposed by Kitamura et al. includes a central needle acting as a source electrode surrounded by six grounding electrodes at 2 mm distance [27]. In a tactile display for presenting spatial electro-vibration stimuli, the subject touched an array of electrodes with 1 mm resolution with his/her fingertip while grasping a grounding metal plate [28]. Electro-tactile interface named Tacttoo comprises eight equispaced circular electrodes (2 mm diameter) arranged into three rows with 4 mm center-to-center spacing [29]. Kajimoto et al. used an electrotactile fingertip display comprising 2 × 5 array of electrodes (1 mm diameter and 2.54 mm distance) [30]. Although all based on same core technology, the presented systems differ in number of electrodes and their configuration, as well as the configuration of the reference electrode. While some systems used the remaining pads from the matrix as reference when one pad is activated [27], [29], [30], none of these studies systematically investigated the distribution of elicited sensations and how this distribution depends on the number and positioning of the pads acting as a reference.

Another relevant aspect of electrotactile stimulation, especially when applied to fingertips, is the polarity of pulses. When considering the monophasic stimulation, previous research suggests that cathodic stimuli produce weak, diffused and blurred sensations, that differ both in magnitude and quality from the sensations produced by anodic stimuli [30], [33]. In addition, anodic stimulation also requires lower current thresholds in fingertips [33], [34]. Yem and Kajimoto showed that anodic and cathodic stimulation produced vibration and pressure sensations, respectively [31], and they combined the two modalities in a tactile feedback device [25]. However, monophasic stimulation can also cause damage to the tissue (cathodic) or the electrode itself (anodic) due to uncompensated charge transfer [35]. To reach a compromise between the two undesirable effects and guarantee safety during prolonged use, this study focuses on symmetrical charge-balanced biphasic stimulation, characterized as very similar to anodic stimulation by Kaczmarek et al. [33].

The present study is a result of the research aiming to achieve natural-like tactile sensations via electrotactile technology by implementing a high-resolution, spatially distributed electrotactile stimulation in a wearable glove that will enrich the VR/AR environment with the tactile sense and thereby provide a new level of immersive experiences. To reach this goal, however, it is necessary to acquire the fundamental knowledge about the psychometric properties of the fingertip stimulation through matrix interfaces, which is still missing in the literature. More specifically, the main goal of the present experiment was to validate novel custom-designed multi-pad electrodes for electrotactile stimulation of fingertips and explore the distribution of sensations elicited by delivering the stimulation through eight individual pads. The latter is particularly important since it reveals if a matrix interface elicits physically congruent sensations that are located below and/or closely around an active pad. An additional unique feature of electrotactile stimulation (versus vibromotors) is that it offers flexibility in selecting active and reference electrodes in order to shape the electrical field within the tissue [36]. Therefore, another important question for the practical application of a matrix interface is how the distribution of sensations is affected by changing the effective size of the reference electrode (i.e., number of pads assigned to the reference), as well as its position (i.e., location of pads comprising the reference) for the given size. We additionally hypothesized that the configuration of the reference electrode could be used as an additional control input to modulate the location and spread of the elicited sensations.

II. Methods

A. Setup

The experimental setup included:

1) Custom-made electrode matrix for index finger,

2) Transparent rubber roll-on garment for securing electrode-skin contact,

3) Multichannel programmable electrical stimulator,

4) Standard tablet PC with a custom-made LabView (National Instruments, USA) application.

Multi-pad electrodes were custom designed as the initial prototypes of the high-density fingertip electrotactile interface. The distribution of electrode pads was chosen according to the fingertip ergonomics, while the shape and size of the individual pads reflect a compromise between maximizing the actuating area to decrease the voltage requirements, routing of the

This article has been accepted for publication in a future issue of this journal, but has not been fully edited. Content may change prior to final publication. Citation information: DOI 10.1109/TOH.2022.3141187, IEEE Transactions on Haptics

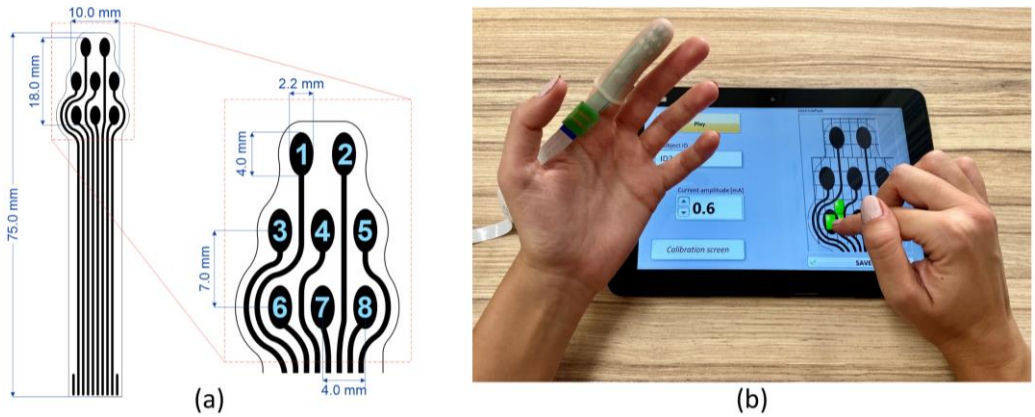

Fig. 1. (a) Technical drawing of the custom-designed electrode for electrotactile stimulation of fingertips, with labelled dimensions and pad numeration. (b) A subject performing the experiment, with the electrode positioned on the non-dominant index finger and secured with transparent silicone cover, while the dominant hand was used for controlling the designated application on the tablet PC.

conductive leads around the pads, and increasing inter-pad distance to improve localization. Eight elliptical pads were distributed in three rows following the finger morphology and ergonomics. As shown in Fig. 1a, the top row covering the narrow part of the fingertip comprised two pads, while the remaining six pads were equally distributed in the middle and bottom rows. The selected dimensions of the pads (4.0 mm major axis × 2.2 mm minor axis) resulted in 7.0 mm^2 conductive surface. The electrodes were manufactured by screen-printing of a conductive medical grade Ag/AgCl layer (Electrodag 6037E SS, Henkel AG & Co. KGaA, DE) on a flexible commercial PET substrate (Electrom Flex, Policrom Screens S.p.A.1, IT). Conductive leads were covered with a dielectric coating (Electrodag PF-455B, Henkel AG & Co. KGaA, DE). Ergonomic design and choice of flexible substrate allowed electrode bending and provided a close contact of the electrode with the skin.

The stimulator unit was used to generate current-controlled rectangular symmetric biphasic pulses with parameters adjusted for electrotactile stimulation of fingertips, with amplitude in the range of 0.1 mA–9 mA (0.1 mA step) and 200 V output voltage. The unit allowed online control of the stimulation parameters and the selection of electrode pads to deliver the stimulation, through a communication protocol with textual commands that could be sent from any device (e.g., tablet PC used in this study) via a Bluetooth communication interface. Hereafter, we denote as "active electrode" a set of pads that is intended to produce tactile sensation, while the "reference electrode" denotes a group of pads selected to close the electrical circuit but which ideally should not elicit tactile sensation. In the present experiment, active electrode always comprised a single pad, as explained below, while the reference included up to 7 pads. Since the stimulation unit produced symmetrical biphasic pulses, the stimuli delivered by the active and reference electrode were identical if the electrodes were of the same size (single pad). However, when the reference electrode was larger (two or more pads) the current density below the reference was lower compared to that below the active pad. An additional factor that could lead to difference in sensations is the "order" in which the pulses were delivered; however, investigating this effect was out of the scope of the presented study.

B. Protocol

Ten healthy volunteers participated in the study (gender: 5/5 female/male, average age: 30.1 ± 10.4 years). All subjects were right-handed, as determined by the Oldfield questionnaire for the assessment of handedness [37]. The subjects had no musculoskeletal or somatosensory disorders, nor visible damages of the skin of the fingertips. Before participating in the experiments, the subjects were provided with an information sheet explaining the methods and objectives of the study. After reading the information, they signed an informed consent form and provided permission for the publication of their photographs for scientific purposes. The study was conducted in accordance with the Declaration of Helsinki and the experimental protocol was approved by the local ethics committee.

The subjects were comfortably seated in front of the table with the tablet PC and the stimulator unit placed in front of them. The electrode was positioned on the fingertip of the non-dominant index finger and fixed with a transparent silicone roll-on garment to secure electrode-skin contact, but also to allow the subjects to see the electrode pads. The electrode was positioned on the non-dominant side so that the subjects could use their dominant index finger for controlling the application via touchscreen of the tablet PC (Fig. 1b). The stimulation frequency and pulse width were set at 30 Hz and 400 μs, respectively. These values were determined through pilot tests as they produced comfortable sensations with gradual modulation of intensity using the amplitude increment of 0.1 mA. The pulse amplitude was individually adjusted for each configuration of active and reference electrode, as explained below.

Each experimental session started with amplitude calibration. The subjects were instructed to adjust the amplitudes for eight electrode pads individually. They selected the pad by touching the appropriate pad on the electrode illustration (the pad was green when active, and black otherwise) and changed the amplitude using the up/down arrows (0.1 mA increment step). They were instructed to adjust the stimulation intensity until they felt clear, comfortable, and localized sensation. The goal of the calibration process was to

introduce the concept of electrotactile fingertip stimulation to the subjects and allow them to map the position of the active pad to the perceived location of the evoked sensation.

During calibration, the reference electrode for the active pads comprised three pads. Locating the reference electrode on the fingertip (i.e., selecting a subset of pads) was inspired by the systems presented in the literature [27], [29], [30] that used similar approach and the decision was also confirmed in a pilot test. This approach was compared to four remote reference electrodes of significantly larger surface positioned at finger dorsum (middle phalanx), center of hand dorsum; center of the of palm and around the wrist. Ten healthy subjects performed a spatial discrimination test which included 200 stimuli (5 reference electrode configurations × 8 active pads × 5 repetitions) distributed in a random order. For each stimulus, subjects adjusted the current amplitude and selected one of the eight pads. The pilot results (Friedman test) showed that the electrode positioned on the finger dorsum resulted in significantly lower mean success rate (58%) compared to the electrodes positioned on the palm (75%) and around the wrist (69%), while there were no significant differences between the remaining configurations (3-pads 67% and hand dorsum 65%). The "embedded" reference was therefore selected as the resulting design is also more compact. When active pad was in the top row (Fig. 1a, pads #1 and #2) and bottom row (Fig. 1a, pads #6, #7 and #8) of the electrode matrix, the reference electrode comprised three pads from the middle row (Fig. 1a, pads #3, #4 and #5). When one of three pads from the middle row was active, the reference electrode comprised three pads from the bottom row. These particular combinations of active pads and 3-pad reference electrodes are denoted as "control configurations", as they also provided orientation and guidance for the subjects, allowing them to map the position of each pad to the region of the fingertip where the sensation was perceived.

The main part of the experimental session was the localization test which included 36 stimuli in a single block lasting approximately 15 minutes. Individual blocks were repeated 10 times (360 stimuli in total), with a break of at least 2 h between the tests to avoid mental fatigue. The electrode was positioned at the beginning and removed at the end of each block. The electrode was carefully placed in the center of the fingertip, but the placement was not marked between the applications in order to mimic the realistic application scenario. Two active pads positioned diagonally in the opposite corners of the electrode matrix (pad #2 in the top-right corner and pad #6 in the bottom-left corner, Fig. 1a) were combined with 15 different reference electrode configurations (2 × 15 = 30 stimuli). In addition, a single block also included six remaining pads with corresponding 3-pad reference electrodes (control configurations). It should be noted that the illustrations of all tested configurations are presented along with the obtained results in Fig. 2 (control configurations), Fig. 4 (pad #2) and Fig. 5 (pad #6), in order to avoid redundancy. The order of 36 tested configurations was randomized in each experimental block, with each configuration being presented only once.

The selected configurations for the two active pads included different sizes and positions of the reference electrode: three positions for one-, two- and three-pad reference, two positions for four- and five-pad reference, and a single position for six- and seven-pad reference electrode. The configurations were selected to vary the distance, orientation, and spatial positioning of the reference electrode in relation to the active pad.

The experiment was double-blinded, with neither the experimenter nor the subject knowing which active/reference electrode configuration was currently being used to deliver the stimulation. Furthermore, the subjects were not given any information on the configurations that will be tested (e.g., active pads) and/or sensations that can be expected. They were instructed that stimuli can appear randomly across the complete electrode surface and that perceived location should be marked. The subjects were presented with the Localization screen, showing the electrode drawing covered with a grid (Fig. 1b). Each electrode pad and its surrounding area were covered with a 3 × 3 grid, resulting in a total of 72 fields extending over the whole surface of the electrode. The subjects activated the experiment by pressing the Play button, adjusted the current amplitude using up/down arrows to obtain comfortable and localized sensation, and then indicated the location of the perceived stimulus by selecting an arbitrary number (one or more) of the fields of the grid. They were instructed to mark all fields associated with the sensation (e.g., one "connected" area or several "disconnected" points). They positioned their non-dominant hand with palm facing up, allowing them to look at their index fingertip and the electrode. The orientation of the physical electrode matched its visual representation on the computer screen, providing a spatial reference when mapping the sensation location using the GUI. Once the subject confirmed his/her selection by pressing the Save button, the active/reference electrode configuration was automatically updated, and another stimulus was presented. The stimulation was continuous, but the subjects were allowed to pause it in any moment by pressing the Play button again.

C. Data analysis

The localization of elicited sensations was represented in the form of heatmaps, where the color indicated how often a particular field in the grid has been selected for each active/reference electrode configuration. In each trial, the intensity of 1/N was assigned to every selected field, where N is the total number of fields selected in that trial. The remaining fields were assigned zero intensity. Therefore, the total intensity of a map representing a single trial was 1. Maps from ten experimental blocks were summed for each subject and each active/reference electrode configuration, thus forming subject-specific configuration heatmaps. Overall configuration heatmaps were formed by summing subject-specific heatmaps for each configuration. Although the theoretical maximum would be 100 (i.e., if all 10 subjects consistently selected only one and the same pad in all 10 experimental blocks), all heatmaps were scaled to the overall maximal intensity to improve the visual representation, resulting in the intensity range from 0 to 40.

In case of eight control configurations comprising active pads combined with 3-pad reference electrodes, three outcome

measures were calculated from the subject-specific configuration heatmaps: X and Y coordinates of the weighted mean, as well as the Euclidean distance between the weighted mean and the active pad, where the coordinates (0,0) corresponded to the bottom left field of the grid, and X and Y are along transversal and longitudinal axis, respectively.

Anderson-Darling test showed that not all data were normally distributed. Therefore, non-parametric tests were employed in the statistical analysis. In order to evaluate if the sensations elicited by the eight active pads were localized to spatially distinct areas of the finger, we assessed if there were statistically significant differences in X and Y coordinates of their subject-specific weighted means. First, we used Kruskal-Wallis test and Mann-Whitney U-test with false discovery rate correction for post-hoc multiple comparisons to compare aggregated Y coordinates of the pads from three different rows of the electrode matrix ({1, 2} vs. {3, 4, 5} vs. {6, 7, 8}). Subsequently, we compared X coordinates for individual pads within each row (1 vs. 2, 3 vs. 4 vs. 5, and 6 vs. 7 vs. 8) using Wilcoxon signed rank test (for the first row with two pads) or Friedman test (for the remaining two rows comprising three pads each). The Euclidean distance from the weighted means to the target active pad, was compared using the Friedman's test to assess the differences in the accuracy of localization between the eight pads.

In case of two active electrode pads (pads #2 and #6) combined with 15 reference electrode configurations, the heatmaps were used for the initial characterization of the localization results. To assess if the localization was affected significantly when changing the position of the reference electrode, we compared the distance along X and Y axes between the subject-specific weighted means and the active pads in the case of 1- and 2-pad reference electrode using the Friedman test.

Next, we have selected a subset of configurations with best localization properties for a more detailed analysis, according to the following steps. The grid field with the highest intensity on the overall heatmap was identified for each configuration, and if it was positioned outside of the 3 × 3 grid surrounding the target active pad, the configuration was omitted from further analysis. For each remaining overall map, we calculated the position of the weighted mean and its Euclidean distance from the center of the active pad (in mm). This distance was used as the outcome measure for selecting one representative configuration in cases when different positions with the same number of reference electrode pads were used, i.e., for configurations with one to five pads. For both active pads (pads #2 and #6), the configurations with minimal Euclidean distance for the given reference electrode size were selected for further analysis, resulting in a subset of seven configurations with the reference electrode comprising one to seven pads. The main outcome measure for comparing (Friedman test) the selected configurations was the distance (in both X and Y axis) between the subject-specific weighted means and the target active pad. In addition, we analyzed the effects of changing the reference electrode size on mean current amplitude.

In all the cases, post-hoc pairwise comparisons were performed using Wilcoxon signed-rank test for paired samples with false discovery rate correction. The threshold for the statistical significance was set at $p < 0.05$.

III. Results

The overall localization heatmaps for the eight control electrode configurations are presented in Fig. 2. The pads of the reference electrode are labelled with the letter "R", while the position of the overall weighted mean is indicated by the red cross. Although there is some spreading of the elicited sensations, which in some cases can be even rather far from the point of stimulation, the sensations were still localized mostly at the active pad. Each heatmap contained a single distinct field with the highest intensity, coinciding with the central area (grid) of the active pad. The intensity, and therefore the influence of the remaining 71 fields was much lower, as indicated by the position of the overall weighted means. All weighted means were positioned within the 3 × 3 grid surrounding the target active pad, except for pad #6 where it was slightly above this area. Two reference pads from the top row (#1 and #2) exhibited

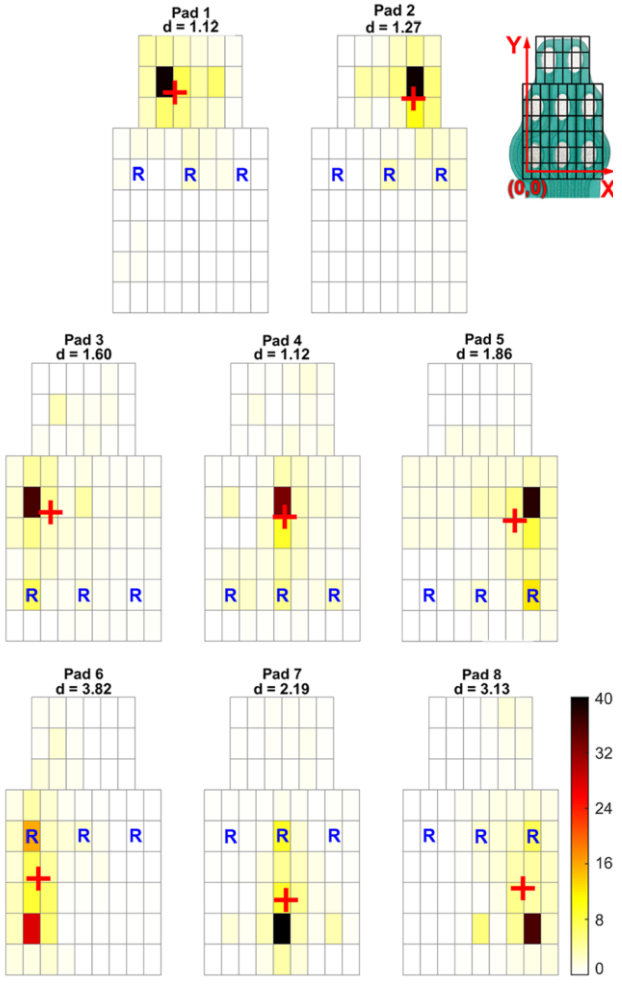

Fig. 2. Overall localization heatmaps, average across ten subjects and ten experimental sessions, for eight control configurations. The heatmaps are arranged following the configuration and numeration of pads on the fingertip electrode (Fig. 1). Reference electrode pads are labelled with the letter "R". The red cross marks the position of the overall weighted mean. Letter "d" indicates the distance from the active pad in mm.

This article has been accepted for publication in a future issue of this journal, but has not been fully edited. Content may change prior to final publication. Citation information: DOI 10.1109/TOH.2022.3141187, IEEE Transactions on Haptics

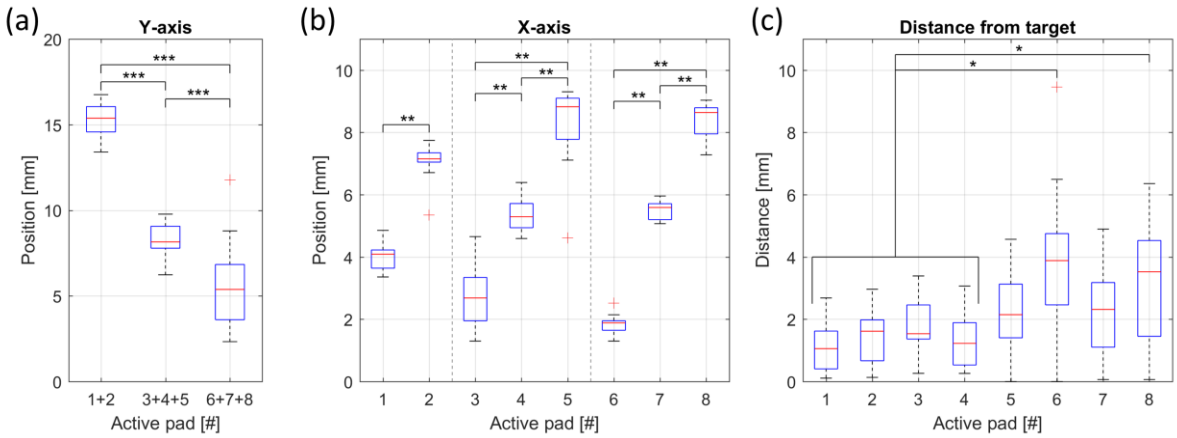

Fig. 3. Boxplots of X-axis (a) and Y-axis (b) position of the subject-specific weighted mean and its Euclidean distance from the target pad (c). The red lines are medians, boxes represent interquartile ranges and the whiskers are min and max values. (*, $p < 0.05$; **, $p < 0.01$; ***, $p < 0.001$)

the highest accuracy (i.e., the darkest shade of the centre target pad) and precision (i.e., lowest number of other selected fields on the grid), with the weighted mean positioned on the border of the central field. Electrode pads from the middle and bottom row were characterized by a larger spread. Nevertheless, in case of the pads from the middle row, the overall weighted mean was still next to the active pad. The dispersion was more pronounced in the bottom pads, where the overall weighted mean was at the edge or even outside the 3 × 3 grid limit around the active pad. It can also be noted that the spread of elicited sensations exhibited a characteristic shape: for the top pads, the spread was circular and focused, around the middle pads, the spread was markedly broader and irregular, and for the bottom pads, it was along the longitudinal (Y) axis of the finger. Furthermore, in all cases, the dispersion seems to tend towards the closest reference pad (particularly expressed in middle and bottom rows).

General conclusions from the heatmaps were confirmed by the statistical analysis of the outcome measures. Boxplots of X (for individual eight pads) and Y (for grouped pads within each row) coordinates of the subject-specific weighted means, and their Euclidean distance from the center of the active pad, are presented in Fig 3. The results of the Kruskal-Wallis test (Fig. 3a) showed that there were statistically significant differences along Y-axis ($p < 0.001$) between the pads from the three rows ({1,2} vs. {3, 4, 5} vs. {6, 7, 8}). In addition, Mann-Whitney U-test and Friedman test with pairwise comparisons revealed that the weighted means for the pads in different columns of each row (Fig. 3b) differed significantly along the X-axis (1 vs. 2 for top row $p = 0.002$; 3 vs. 4 vs. 5 for middle row $p < 0.001$, 6 vs. 7 vs. 8 for bottom row $p < 0.001$). For the Y positions (Fig. 3a), the distributions for two top pads were concentrated "far" from those of the middle and bottom pads, whereas the latter were closer to each other and even expressed some overlap (note that the physical distance between the pads along the Y-axis was in fact equal). However, the data distributions for the X position were clearly separated across the columns (Fig. 3b). Therefore, the subjects perceived the eight active pads in different parts of their fingertips, and the two top pads seemed to be best spatially separated from the rest of the electrode. The localization accuracy, assessed as the distance between the subject-specific weighted means and the center of the target pad, complements the information disclosed by the heatmaps (Fig. 3c). The distance increased with active pads moving away from the tip of the fingertip, with median (interquartile range) distance ranging from 1.1 (1.2) mm for pad #1 to 3.9 (2.3) mm for pad #6. Moreover, the minimal values ranged from 0 mm (pads #5 and #6) to 0.26 mm (pads #3 and #4), suggesting that certain subjects managed to achieve an exceptional accuracy. Additionally, the accuracy for two lateral pads (#3 and #5 in the middle and #6 and #8 in the bottom row) was lower compared to that of pads #4 and #7 from the central column. Friedman test showed that these differences for eight reference pads were statically significant ($p = 0.013$), while the pairwise comparisons revealed that the localization accuracy was better for pads #1-4 compared to pads #6 and #8. Note also that the dispersion of the Y-coordinates and the distance of the weighted means across subjects tends to increase from pad #1 to pad #8.

Overall heatmaps for active pads #2 and #6 and different reference electrode configurations are shown in Fig. 4 and Fig. 5, respectively. Heatmaps are arranged in a matrix with seven columns and three rows. Configurations with different reference electrode sizes (1 to 7 pads) are distributed in seven columns. Within each column, the configurations with different positions of the equally sized reference electrode are distributed in separate rows, ranging from three (for the first three reference electrode sizes) to one (for the last two reference electrode sizes). The pad with the highest intensity within each heatmap is surrounded by a black rectangle. Euclidean distance d of the overall weighted mean (labelled with the red cross) from the center of the target active pad is reported above each heatmap (expressed in mm).

For pad #2, changing the size and position of the reference electrode seems to have an effect for the sizes of 1 and 2-pads, while from 3 and more pads, the changes in the reference electrode does not affect the position of the weighted mean (Fig 4). The changes in localization were however more pronounced for pad #6. In this case, increasing the size (rows in Fig. 5) and the position (columns in Fig. 5) shifted the location of the overall weighted mean. This was mostly related to the position along the Y-axis. The shifts in the position were again most expressed for smaller sizes of the reference electrode (1-3

This article has been accepted for publication in a future issue of this journal, but has not been fully edited. Content may change prior to final publication. Citation information: DOI 10.1109/TOH.2022.3141187, IEEE Transactions on Haptics

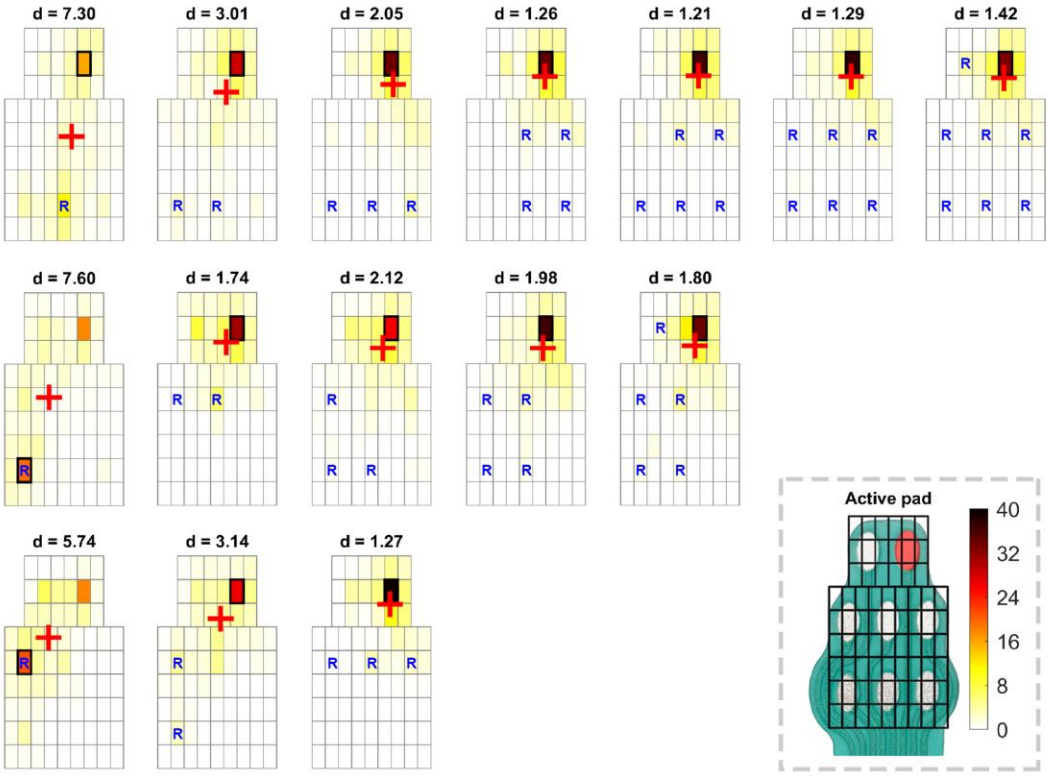

Fig. 4. Overall heatmaps of 15 configurations with different size (columns) and positions (rows) of the reference electrode for active pad #2. Reference electrode pads are labelled with the letter "R". Red cross denotes the overall weighted mean, while its Euclidean distance from the active pad is reported above each map (in mm). The highest intensity pad within each map is surrounded by a black rectangle.

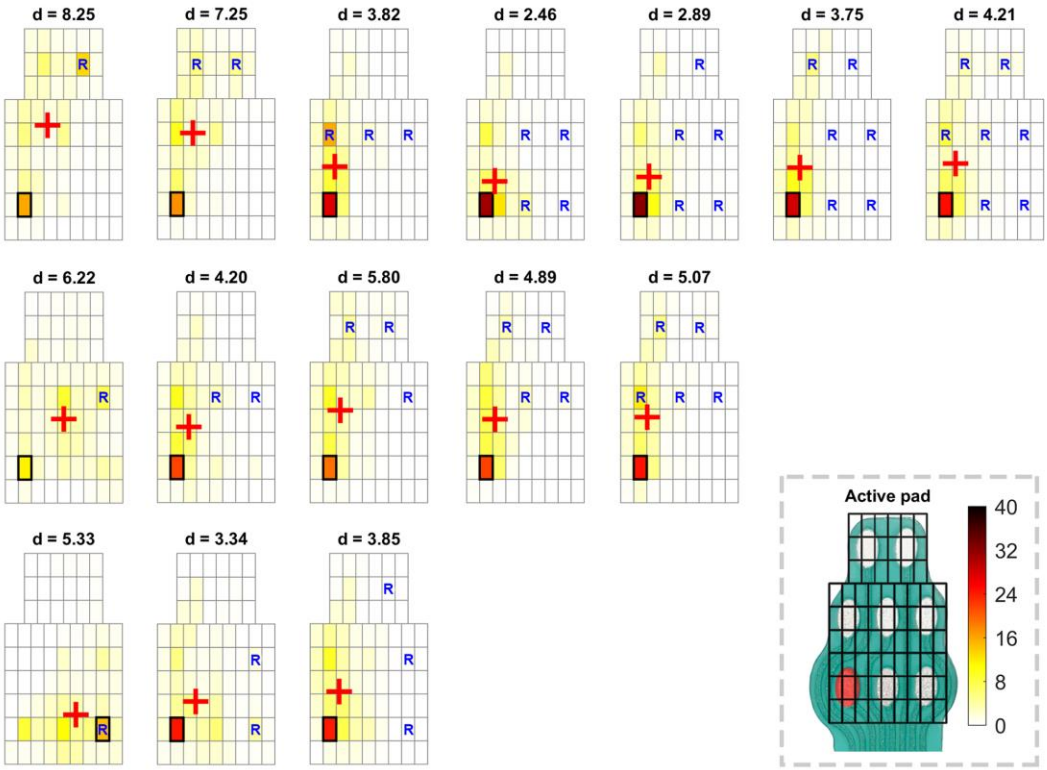

Fig. 5. Overall heatmaps of 15 configurations with different size (columns) and positions (rows) of the reference electrode for active pad #6. Reference electrode pads are labelled with the letter "R". Red cross denotes the overall weighted mean, while its Euclidean distance from the active pad is reported above each map (in mm). The highest intensity pad within each map is surrounded by a black rectangle.

pads). In particular, for a single pad reference, changing the position "shifts" the overall distribution of the reported sensations (yellow color). For instance, in Fig. 5 first column, the distribution moves from the top of the fingertip (first row),

This article has been accepted for publication in a future issue of this journal, but has not been fully edited. Content may change prior to final publication. Citation information: DOI 10.1109/TOH.2022.3141187, IEEE Transactions on Haptics

through the middle (second row), and then to the bottom area (third row). The accuracy in localization is overall better for pad #2 compared to pad #6, as the overall weighted mean is closer to the active pad. It should be noted that for both pads #2 and #6 when considering 1-pad reference electrode, the field with the highest intensity was for some configurations in the center of the active pad and for others in the center of reference pad. However, for all other sizes and positions of the reference electrode, it was in the center of an active pad.

The results of the analysis of the subset of configurations with the best localization are presented in Fig. 6 (active pad #2) and Fig. 7 (active pad #6). Subject specific weighted means are presented in the top panel (colored crosses). Boxplots of the distances between the weighted means and the center of the active pad along the X- and Y-axis are shown in left and right bottom plots, respectively. The distance is negative if the weighted mean was positioned left from (X distance) and below the centre of the active pad (Y distance). The results of Friedman's test showed that statistically significant differences between seven selected reference electrode configurations were

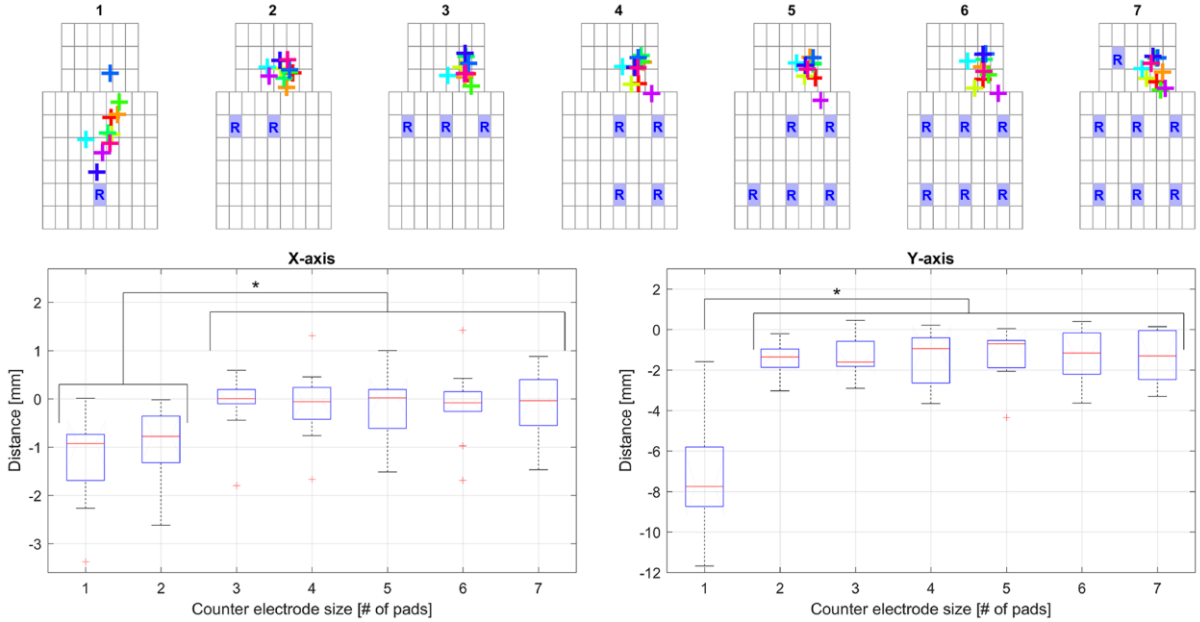

Fig. 6. Summary results for active pad #2 and seven selected reference electrode configurations. Top: Subject-specific weighted means (marked with a cross of a different color for each subject) for seven selected configurations with increasing reference electrode size (from left to right). Bottom: Distance between weighted means and the center of the active pad along X-axis (left) and Y-axis (right). Horizontal bars with asterisks indicate the statistically significant difference in median distance between the respective conditions (reference electrode size). (*, $p < 0.05$)

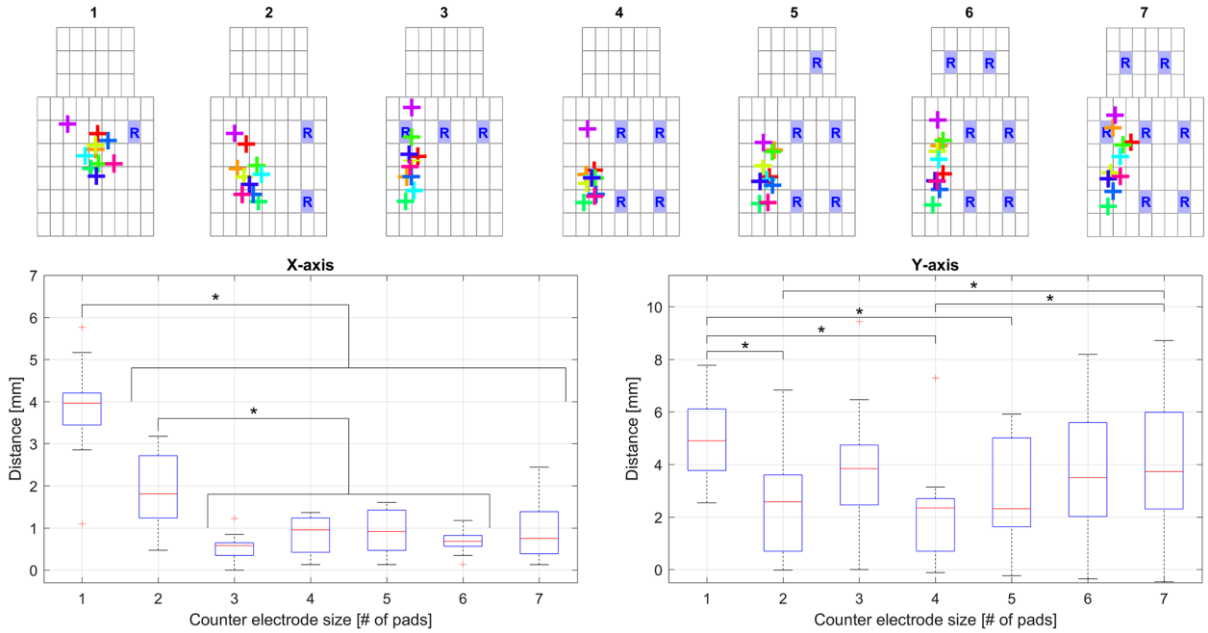

Fig. 7. Summary results for active pad #6 and seven selected reference configurations. Top: Subject-specific weighted means (marked with a cross of a different color for each subject) for seven selected configurations with increasing reference electrode size (from left to right). Bottom: Distance between weighted means and the center of the active pad along X-axis (left) and Y-axis (right). Horizontal bars with asterisks indicate the statistically significant difference in median distance between the respective conditions (reference electrode size). (*, $p < 0.05$)

This article has been accepted for publication in a future issue of this journal, but has not been fully edited. Content may change prior to final publication. Citation information: DOI 10.1109/TOH.2022.3141187, IEEE Transactions on Haptics

present for both active pads and in both directions (pad #2: X-axis $p < 0.001$, Y-axis $p = 0.008$; pad #6: X-axis $p < 0.001$, Y-axis $p = 0.003$). The results of pairwise comparisons are indicated in the boxplots with horizontal bars and asterisks. The summary results reflect the qualitative observations in Fig. 4 and Fig. 5. The only significant difference in the position of the weighted mean for pad #2 was between 1- and 2-pad sizes versus the other sizes. For pad 6#, the differences followed the same trend for X-axis; however, Y distance of the weighted mean was significantly affected in more cases. For instance, the weighted mean was significantly closer to the active pad for 4-pad compared to 1- and 7-pad reference electrode. The stimulation amplitude was not significantly affected by the size of the reference electrode in case of both pads.

The effects of changing the position of the reference electrode while maintaining the same size are illustrated in Fig. 8 for 1- and 2-pad reference electrode. The two sizes (1- and 2-pad) were selected because the effect was most expressed (Fig. 4 and Fig. 5) in these cases. For both active pads, the differences among the three configurations were most prominent in the case of a single pad reference electrode. Moving the reference electrode significantly changed the distance of the weighted mean along the X-axis only in the case of a single pad reference. The weighted mean shifted significantly along the Y-axis for both 1- and 2-pad reference, and this effect was more expressed for pad #6. The shifts of the weighted mean approximately corresponded to the movement of the reference electrode along the X- and Y-axis. For instance, for both active pads #2 and #6, the distance of the weighted mean along X-axis was significantly different for the first configuration with a single pad compared to the remaining two, since in this case the reference was horizontally closest to the active pad.

IV. Discussion

We have designed and developed a novel flexible multi-pad electrode for the stimulation of fingertips, as a first step towards high-density wearable electrotactile interface covering complete hand. The electrodes were evaluated in terms of localization of stimuli delivered to eight electrode pads in ten healthy subjects, who repeated the experimental session ten times each. Additionally, we investigated the influence of the size and positioning of the reference electrode on the localization of sensations perceived under single active electrode pad. To that aim, we tested fifteen different reference electrode configurations for two active electrode pads positioned in the opposite corners of the electrode matrix.

The electrode design consists of eight elliptical pads arranged into three rows, with the two pads in the top row and three pads in the remaining two rows. A similar configuration was proposed by Withana et al. for 8 circular pads with 2 mm diameter equidistantly distributed within a tattoo-like matrix electrode [29]. However, we opted for slightly larger pads (4.0 mm × 2.2 mm ellipse), which resulted with an increased actuating area (18.0 mm × 10.0 mm, as shown in Fig. 1a, compared to 10.0 mm × 10.0 mm in [29]), still aligned to the ergonomics and dimensions of an adult's fingertip [38].

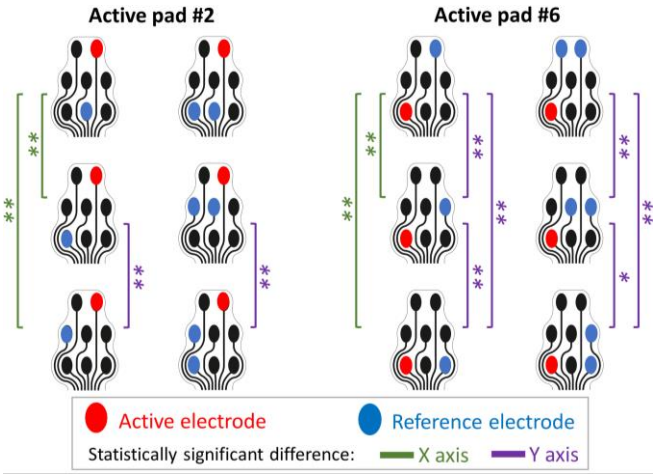

Fig. 8. The statistical analysis of the shifts in the distance of the subject-specific weighted means along X and Y axis for pads #2 and #6 depending on the position of the one and two pad reference electrodes. The corresponding heatmaps are presented in Figure 5 (active pad #2) and Figure 6 (active pad #6). (*, $p < 0.05$; **, $p < 0.01$)

Electrode dimensions were chosen to allow fitting eight pads within one-size-fits-all solution and by considering the hardware limitations of the stimulation unit. The stimulation system used in this research is based on spatio-temporal distribution of pulses through high voltage switching circuitry, which in turn limits the output voltage to 200 V. This switching technology was selected to allow further development of a high-density (>32 channels), compact and wearable stimulation system, but it also sets some limitations on the pad and hence electrode size, as explained in section II.A. Nevertheless, the proposed electrode design still fulfils general recommendations from Szeto et al. [39], suggesting that the best quality of sensation was obtained when stimulating mechanoreceptors with an active electrode surface ranging from 7 mm^2 to 15 mm^2. Center-to-center distances between two pads (7 mm vertical and 4 mm horizontal, as shown in Fig. 1a) were chosen in an attempt to accommodate different values of two-point discrimination threshold (TPDT) in fingertips reported in the literature. The reported ranges span from 1.00 mm-2.00 mm [1] to 3.80 mm for women and 7.80 mm for men [40] in case of mechanical stimulation, and from 2.00 mm-4.00 mm [41] to 7.25 mm for electrotactile stimulation [42].

The localization test with eight active pads indicated a high accuracy in mapping the stimulus location (Fig. 2), which was corroborated by the subsequent statistical analysis (Fig. 3). Each heatmap was characterized with a single high-intensity field, located in the center of the active electrode pad, and the weighted mean that was positioned nearby. Weighted mean positions for all pads were significantly different along either Y-axis (for pads from three rows of electrode matrix) or X-axis (for pads from different columns of each row), thus showing that the locations of the sensations elicited by the eight active pads were clearly spatially separated. Weighted means for pads #1-4 were significantly closer to the center of respective active pads compared to pads #6 and #8. This is in agreement with the results of the other test where the top of the fingertip resulted in better and more consistent localization compared to the bottom

(e.g., compare pad #2 to pad #6 in Fig. 4 – Fig. 8). This is probably due to a higher density of RA and SA I mechanoreceptive units in the distal parts of the fingertip, which account for spatial acuity [43].

Importantly, in the present study the subjects were not tested using the standard spatial discrimination procedure, including familiarization and reinforced learning prior to the final test [32]. The subjects were not asked to choose among eight possible pads but to freely mark the area where they perceived the stimuli, without any knowledge about the currently tested active/reference electrode configurations. The grid that the subjects used to select the fields also included the electrode pads (Fig. 1b). This was required so that the subjects could map the scheme in the GUI to the physical area of the finger. However, this could have biased the subjects during the field selection. Nevertheless, the effect of the bias was likely minimal (if any) as the subjects did not know which pad was activated during the experiment and they were explicitly asked to faithfully describe the distribution of elicited sensations and not to identify an active pad. This is in fact a critical test since it reveals the "physical" mapping between the delivered stimulation and the perceived sensation. In the spatial discrimination test, the subjects are trained to recognize the active pad and for this, they can use perceptual properties other than the actual physical location, for instance, the difference in intensity and/or quality of sensations elicited by different pads. While this facilitates "conscious" recognition of the active pad, it does not guarantee spatial congruence. For example, the subject can recognize that a pad is active despite the fact that the sensation can be located far from the physical location of the pad on the fingertip.

The tests performed in the present study have demonstrated that there is indeed a spatial "match" between the stimulation and the elicited sensations. However, this is not without its challenges, as the sensation sometimes reached further "outside" of the actual pad. In addition, the tests demonstrate that the spatial distance in the perceptual space can be substantially different from that in the physical space [44]. The physical distance between the rows of the electrode pad was equal, while the perceived location of the first row was further apart from the second row compared to the distance between the second and the third row. Future work will investigate methods to improve the precision of localization. Importantly, in application of interest the subject will use the glove within VR where they will also receive visual feedback on the point of contact and this input might spontaneously bias the tactile perception and thereby increase the precision.

The obtained results for two active pads (#2 and #6) suggested that both the size and position of the reference electrode affected the localization of the perceived stimuli. Moving the small sized (1- and 2-pad) reference electrode produced significant shifts in the location of the elicited sensations in both tested pads. In these cases, the sensation was positioned between the reference and active pads. The results suggest that this approach could be used for the controlled modulation of the perceived sensations and should be systematically explored. In that sense, the location and the size of the reference could be used as an additional parameter (together with frequency and intensity) to shape the properties of the tactile feedback delivered to the fingertip, potentially steering the location with sub-pad resolution.

Increasing the size of the reference electrode produced markedly different effects on the two pads. For pad #2, starting from three-pad reference, the size and position of the reference no longer affected the localization. In all the cases, the weighted mean was located in average less than 1 mm from the centre of the pad in both horizontal and vertical direction. In case of active pad #6, on the contrary, the sensations were systematically shifted towards the top of the fingertip, although the highest "intensity" was still focused around the active pad. Interestingly, the localization did not improve for pad #6 when increasing the size of the reference electrode. Larger size decreases the current density below the reference electrode, but contrary to expectations, this did not affect the localization below the active pad. Therefore, for some specific locations on the proximal parts of the phalange the localization cannot be significantly improved by increasing the surface of the reference electrode. Characterization of additional electrode pads (e.g., pad #4, positioned centrally) would allow determining if the observed differences between pads #2 and #6, which are positioned diagonally in the opposite corner of the electrode matrix, reflect some "discrete" phenomena or more gradual changes across the matrix.

It should be noted that certain subject-specific variability in the presented results could be induced by inconsistent positioning of the electrode throughout ten experimental blocks. The electrode was carefully placed over the central part of the fingertip at the beginning of each block, but the exact positioning was not marked. This decision in the protocol design was made to reflect limitations of the defined application scenario, wherein high-density electrotactile feedback electrodes will be embedded in a glove for VR/AR interaction. Therefore, the calibration procedure was designed to allow subjects to compensate potential mismatches in electrode positioning by mapping the positions of the pads at the beginning of each block (see Methods, controlled configurations). The effect of placement variability was further alleviated by using aggregated results from ten repetitions.

Localization of electrotactile stimuli on the fingers was examined by Higashiyama and Hayashi [45], focusing on the effects of the electrode configuration (concentric vs. unifocal with the reference electrode placed on the instep of the foot) and the body axis (longitudinal vs. transversal). Using nine electrodes positioned on the segments (tip, middle and base) of three fingers (index, middle and ring), the authors showed that the longitudinal electrode placement induced sensory shift, with significantly smaller localization errors for concentric configuration. The concentric configuration used by Higashiyama and Hayashi, with both active and reference electrode positioned on the same finger segment, is comparable to the configurations used in the present study. In addition, the obtained results confirmed that shift in localization is more pronounced along vertical (i.e., longitudinal) axis, especially for active pad #6 (Figs. 5 and 7).

The high precision in spatial localization of stimuli delivered to the fingertips through the presented electrotactile interface without any prior training is an encouraging result. In the following work, we aim to leverage the resolution of our interface and the possibility of simultaneous spatial, frequency and intensity modulation in order to provide the users with intuitive and reliable feedback via custom-designed dynamic stimulation patterns that will communicate relevant interaction through natural-like touch sensations. The present work is an important step towards this goal, as it demonstrates that 3-pad reference elicits localized sensations while 1-pad reference can be used to modulate the location. For instance, a moving sensation could be realized by activating the pads in combination with their associated 3-pad reference electrodes in fast succession. The results however also point out that the quality of localization depends on the pad positioning (top vs. bottom of the fingertip), which can have an impact when generating and perceiving such electrotactile "movements".

ACKNOWLEDGMENT

The authors would like to acknowledge the work of all the partners in the TACTILITY project which enabled us to do the research presented in this manuscript. We thank all the healthy volunteers that participated in our study.

REFERENCES

[1] S. J. Lederman and R. L. Klatzky, 'Haptic perception: A tutorial', *Atten. Percept. Psychophys.*, vol. 71, no. 7, pp. 1439–1459, 2009.

[2] P. Beckerle *et al.*, 'Feel-good robotics: requirements on touch for embodiment in assistive robotics', *Front. Neurorobotics*, vol. 12, p. 84, 2018.

[3] 'TACTILITY – An EU H2020 Research and Innovation Action'. https://tactility-h2020.eu/ (accessed Jan. 14, 2021).

[4] 'Full body haptic feedback & motion capture tracking VR suit', *TESLASUIT*. https://teslasuit.io/ (accessed Jan. 14, 2021).

[5] C. Pacchierotti, S. Sinclair, M. Solazzi, A. Frisoli, V. Hayward, and D. Prattichizzo, 'Wearable haptic systems for the fingertip and the hand: taxonomy, review, and perspectives', *IEEE Trans. Haptics*, vol. 10, no. 4, pp. 580–600, 2017.

[6] K. A. Kaczmarek, J. G. Webster, P. Bach-y-Rita, and W. J. Tompkins, 'Electrotactile and vibrotactile displays for sensory substitution systems', *IEEE Trans. Biomed. Eng.*, vol. 38, no. 1, pp. 1–16, 1991.

[7] A. Y. Szeto and F. A. Saunders, 'Electrocutaneous stimulation for sensory communication in rehabilitation engineering', *IEEE Trans. Biomed. Eng.*, no. 4, pp. 300–308, 1982.

[8] G. C. Burdea and F. P. Brooks, 'Force and touch feedback for virtual reality', 1996.

[9] O. A. Van der Meijden and M. P. Schijven, 'The value of haptic feedback in conventional and robot-assisted minimal invasive surgery and virtual reality training: a current review', *Surg. Endosc.*, vol. 23, no. 6, pp. 1180–1190, 2009.

[10] D. A. Kontarinis and R. D. Howe, 'Tactile display of vibratory information in teleoperation and virtual environments', *Presence Teleoperators Virtual Environ.*, vol. 4, no. 4, pp. 387–402, 1995.

[11] I. Sarakoglou, N. Garcia-Hernandez, N. G. Tsagarakis, and D. G. Caldwell, 'A high performance tactile feedback display and its integration in teleoperation', *IEEE Trans. Haptics*, vol. 5, no. 3, pp. 252–263, 2012.

[12] C. Pacchierotti, D. Prattichizzo, and K. J. Kuchenbecker, 'Cutaneous feedback of fingertip deformation and vibration for palpation in robotic surgery', *IEEE Trans. Biomed. Eng.*, vol. 63, no. 2, pp. 278–287, 2015.

[13] A. Israr, S.-C. Kim, J. Stec, and I. Poupyrev, 'Surround haptics: tactile feedback for immersive gaming experiences', in *CHI'12 Extended Abstracts on Human Factors in Computing Systems*, 2012, pp. 1087–1090.

[14] E. Hoggan, S. A. Brewster, and J. Johnston, 'Investigating the effectiveness of tactile feedback for mobile touchscreens', in *Proceedings of the SIGCHI conference on Human factors in computing systems*, 2008, pp. 1573–1582.

[15] S. Jang, L. H. Kim, K. Tanner, H. Ishii, and S. Follmer, 'Haptic edge display for mobile tactile interaction', in *Proceedings of the 2016 CHI Conference on Human Factors in Computing Systems*, 2016, pp. 3706–3716.

[16] C. Antfolk, C. Balkenius, G. Lundborg, B. Rosén, and F. Sebelius, 'Design and technical construction of a tactile display for sensory feedback in a hand prosthesis system', *Biomed. Eng. Online*, vol. 9, no. 1, p. 50, 2010.

[17] S. Dosen *et al.*, 'Multichannel electrotactile feedback with spatial and mixed coding for closed-loop control of grasping force in hand prostheses', *IEEE Trans. Neural Syst. Rehabil. Eng.*, vol. 25, no. 3, pp. 183–195, 2016.

[18] L. A. Jones and N. B. Sarter, 'Tactile displays: Guidance for their design and application', *Hum. Factors*, vol. 50, no. 1, pp. 90–111, 2008.

[19] Y. Kim, J. Cha, I. Oakley, and J. Ryu, 'Exploring tactile movies: An initial tactile glove design and concept evaluation', *Ieee Multimed.*, 2009.

[20] U. Gollner, T. Bieling, and G. Joost, 'Mobile Lorm Glove: introducing a communication device for deaf-blind people', in *Proceedings of the sixth international conference on tangible, embedded and embodied interaction*, 2012, pp. 127–130.

[21] X. Yu *et al.*, 'Skin-integrated wireless haptic interfaces for virtual and augmented reality', *Nature*, vol. 575, no. 7783, pp. 473–479, 2019.

[22] M. Azadi and L. A. Jones, 'Vibrotactile actuators: Effect of load and body site on performance', in *2014 IEEE Haptics Symposium (HAPTICS)*, 2014, pp. 351–356.

[23] M. Štrbac *et al.*, 'Integrated and flexible multichannel interface for electrotactile stimulation', *J. Neural Eng.*, vol. 13, no. 4, p. 046014, 2016.

[24] R. S. Dahiya, G. Metta, M. Valle, and G. Sandini, 'Tactile sensing—from humans to humanoids', *IEEE Trans. Robot.*, vol. 26, no. 1, pp. 1–20, 2009.

[25] V. Yem and H. Kajimoto, 'Wearable tactile device using mechanical and electrical stimulation for fingertip interaction with virtual world', in *2017 IEEE Virtual Reality (VR)*, 2017, pp. 99–104.

[26] J. Hummel *et al.*, 'A lightweight electrotactile feedback device for grasp improvement in immersive virtual environments', in *2016 IEEE Virtual Reality (VR)*, 2016, pp. 39–48.

[27] N. Kitamura, J. Chim, and N. Miki, 'Electrotactile display using microfabricated micro-needle array', *J. Micromechanics Microengineering*, vol. 25, no. 2, p. 025016, 2015.

[28] H. Ishizuka, K. Suzuki, K. Terao, H. Takao, and F. Shimokawa, 'Development of high resolution electrostatic tactile display', in *2017 International Conference on Electronics Packaging (ICEP)*, 2017, pp. 484–486.

[29] A. Withana, D. Groeger, and J. Steimle, 'Tacttoo: A thin and feel-through tattoo for on-skin tactile output', in *Proceedings of the 31st Annual ACM Symposium on User Interface Software and Technology*, 2018, pp. 365–378.

[30] H. Kajimoto, N. Kawakami, T. Maeda, and S. Tachi, 'Electro-tactile display with force feedback', in *Proc. World Multiconference on Systemics, Cybernetics and Informatics (SCI2001)*, 2001, vol. 11, pp. 95–99.

[31] V. Yem and H. Kajimoto, 'Comparative evaluation of tactile sensation by electrical and mechanical stimulation', *IEEE Trans. Haptics*, vol. 10, no. 1, pp. 130–134, 2016.

[32] J. Malešević, M. Isaković, M. A. Garenfeld, S. Došen, and M. Štrbac, 'The Impact of Stimulation Intensity on Spatial Discrimination with Multi-Pad Finger Electrode', *Appl. Sci.*, vol. 11, no. 21, p. 10231, 2021.

[33] K. A. Kaczmarek, M. E. Tyler, and P. Bach-y-Rita, 'Electrotactile haptic display on the fingertips: Preliminary results', in *Proceedings of 16th Annual International Conference of the IEEE Engineering in Medicine and Biology Society*, 1994, vol. 2, pp. 940–941.

[34] K. A. Kaczmarek, M. E. Tyler, A. J. Brisben, and K. O. Johnson, 'The afferent neural response to electrotactile stimuli: preliminary results', *IEEE Trans. Rehabil. Eng.*, vol. 8, no. 2, pp. 268–270, 2000.

[35] D. R. Merrill, M. Bikson, and J. G. Jefferys, 'Electrical stimulation of excitable tissue: design of efficacious and safe protocols', *J. Neurosci. Methods*, vol. 141, no. 2, pp. 171–198, 2005.

[36] H. Kajimoto, N. Kawakami, S. Tachi, and M. Inami, 'Smarttouch: Electric skin to touch the untouchable', *IEEE Comput. Graph. Appl.*, vol. 24, no. 1, pp. 36–43, 2004.
[37] R. C. Oldfield, 'The assessment and analysis of handedness: the Edinburgh inventory', *Neuropsychologia*, vol. 9, no. 1, pp. 97–113, 1971.
[38] K. Dandekar, B. I. Raju, and M. A. Srinivasan, '3-D finite-element models of human and monkey fingertips to investigate the mechanics of tactile sense', *J Biomech Eng*, vol. 125, no. 5, pp. 682–691, 2003.
[39] A. Y. Szeto, R. R. Riso, R. V. Smith, and J. H. Leslie, 'Sensory feedback using electrical stimulation', in *Rehabilitation engineering*, CRC Press, 1990, p. 29.
[40] N. J. Davey, A. V. Nowicky, and R. Zaman, 'Somatotopy of perceptual threshold to cutaneous electrical stimulation in man', *Exp. Physiol.*, vol. 86, no. 1, pp. 127–130, 2001.
[41] K. Hayashi and T. Ninjouji, 'Two-point discrimination threshold as a function of frequency and polarity at fingertip by electrical stimulation', in *The 26th Annual International Conference of the IEEE Engineering in Medicine and Biology Society*, 2004, vol. 2, pp. 4256–4259.
[42] M. Solomonow, J. Lyman, and A. Freedy, 'Electrotactile two-point discrimination as a function of frequency, body site, laterality, and stimulation codes', *Ann. Biomed. Eng.*, vol. 5, no. 1, pp. 47–60, 1977.
[43] R. S. Johansson and A. B. Vallbo, 'Tactile sensibility in the human hand: relative and absolute densities of four types of mechanoreceptive units in glabrous skin.', *J. Physiol.*, vol. 286, no. 1, pp. 283–300, 1979.
[44] M. R. Longo and P. Haggard, 'Weber's illusion and body shape: anisotropy of tactile size perception on the hand.', *J. Exp. Psychol. Hum. Percept. Perform.*, vol. 37, no. 3, p. 720, 2011.
[45] A. Higashiyama and M. Hayashi, 'Localization of electrocutaneous stimuli on the fingers and forearm: effects of electrode configuration and body axis', *Percept. Psychophys.*, vol. 54, no. 1, pp. 108–120, 1993.

Milica Isaković received her BSc and MSc degrees from the University of Belgrade, School of Electrical Engineering in 2014 and 2015, respectively. She started PhD studies at the same faculty in 2015, exploring the use of electrical stimulation for providing feedback from myoelectric hand prostheses, and defended her PhD thesis in 2020.

She joined Tecnalia Serbia Ltd in 2014 and is currently a Senior Researcher. From 2016 to 2020, she was also engaged in the research project of the Ministry of Education, Science and Technological Development of the Republic of Serbia, as a Research Assistant at the School of Electrical Engineering. Her research interests include electrotactile stimulation in assistive devices for neurorehabilitation, myoelectric control and biomedical signal processing.

Jovana Malešević received undergraduate (2011) and master's degree (2012) in Electrical Engineering from University of Belgrade, Serbia. She started PhD studies at University of Belgrade, department of Biomedical Engineering and Technology in 2014 and defended her PhD thesis in 2020.

In 2012 she joined Tecnalia Serbia Ltd. Since then she has been working on projects related to design and development of electrical stimulation systems for lower- and upper-limb neurorehabilitation, and currently holds position of a Senior Researcher. Her research interest includes systems for limb control based on electrical stimulation, limb kinematics analysis and electrotactile feedback.

Miloš Kostić received his undergraduate degree, master's degree and PhD in Electrical Engineering from University of Belgrade, Serbia in 2009, 2010 and 2014 respectively. He specialized in neurorehabilitation technologies, while the focus of his PhD research was rehabilitation robotics.

In 2014, he joined the Health Department of Tecnalia Research and Innovation in San Sebastián (Spain) as a Lead Reserecher. In 2017 he transferred to Tecnalia Serbia Ltd. as a Senior Researcher on projects related to development and testing of hybrid clinical systems based on electrical stimulation. His primary research interests are in electrical stimulation, quantitative multimodal assessment and improvement of early user involvement development methodologies.

Strahinja Došen (Member, IEEE) received the Diploma of Engineering degree in electrical engineering and the M.Sc. degree in biomedical engineering in 2000 and 2004, respectively, from the Faculty of Technical Sciences, University of Novi Sad, Serbia, and the Ph.D. degree in biomedical engineering from Aalborg University, Aalborg, Denmark, in 2009.

Between 2011 and 2017, he was a Research Scientist with the University Medical Center Göttingen, Georg-August University, Germany. He is currently an Associate Professor at the Department of Health Science and Technology, Aalborg University. He has published more than 65 manuscripts in peer-reviewed journals in the field of biomedical engineering. His research interests include movement restoration and control, rehabilitation robotics, sensory feedback and human-machine interfacing for sensory-motor integration.

Dr. Dosen is a member of IEEE EMBS. He is currently an Associate Editor for the Journal of NeuroEngineering and Rehabilitation, and Frontiers in Bioengineering and Biotechnology.

Matija Štrbac received B.Sc. and M.Sc. degrees from the University of Belgrade, School of Electrical Engineering in 2010 and 2011, respectively. In 2011, he enrolled PhD studies at the same faculty with the focus on the development of the computer vision system for automatic control of electrical stimulation and defended his thesis in 2017.

From 2012 until 2015, he worked on the project financed by the Ministry of Education, Science and Technological Development of the Republic of Serbia as a Research Assistant at the School of Electrical Engineering. From 2013, he started working for Tecnalia Serbia Ltd. as the Lead Researcher in the projects related to FES assisted rehabilitation of upper extremity and development of electrotactile feedback interface for myoelectric hand prostheses. Since 2016 he is the Director of Tecnalia Serbia Ltd.